



Gain suppression mechanism in LGADs and SEE studies in a RD53B chip measured with the TPA-TCT method

Esteban Currás¹, Marcos Fernández García^{1,2}, Michael Moll¹, Raúl Montero³, Rogelio F. Palomo⁴, Sebastian Pape^{1,5}, Ivan Vila², Moritz Wiehe^{1,6}

¹CERN

²Instituto de Física de Cantabria

³Universidad del País Vasco (UPV-EHU)

⁴Universidad de Sevilla

⁵TU Dortmund University

⁶Universität Freiburg

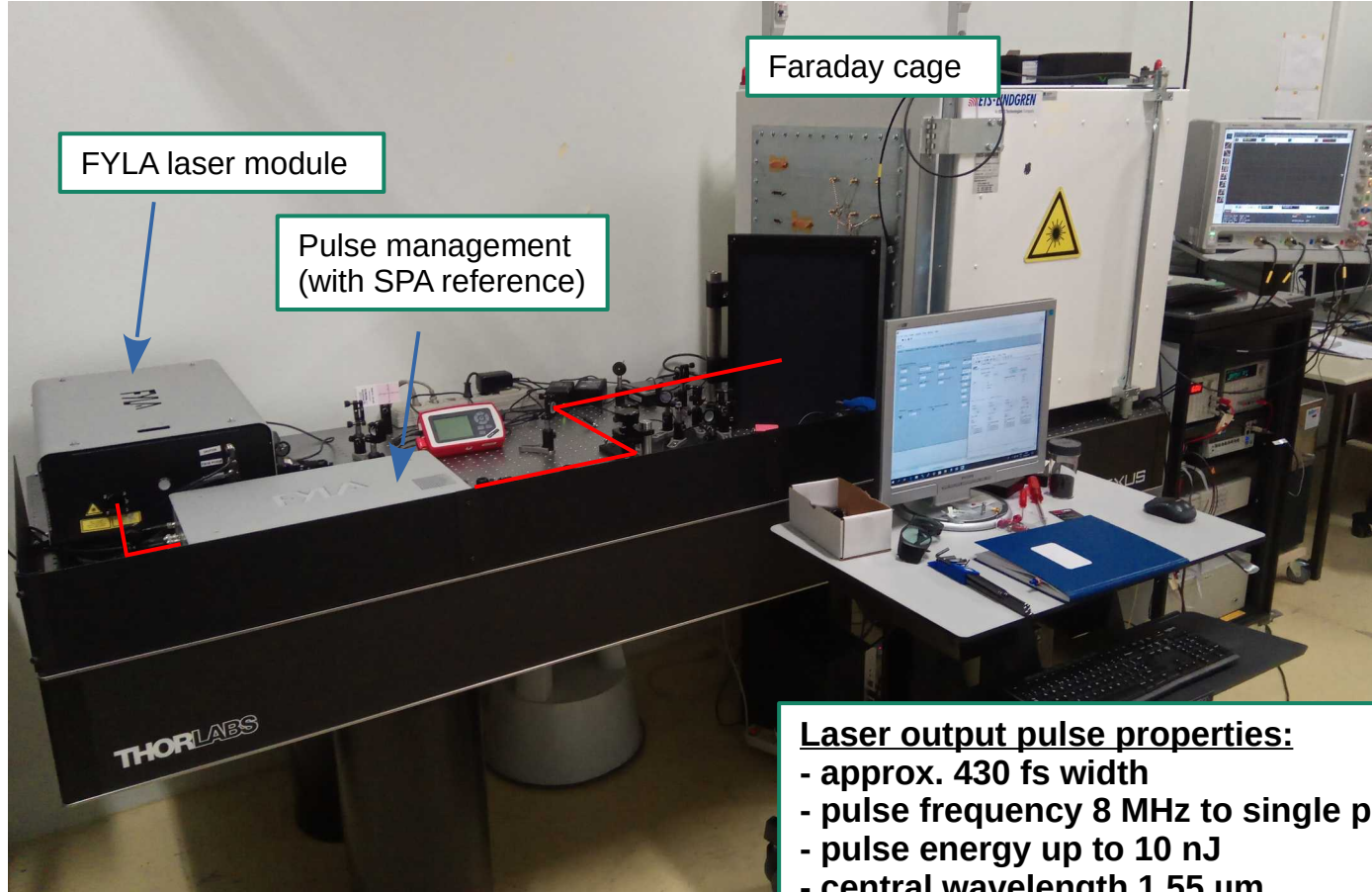


Outline

- **The TPA-TCT setup at CERN SSD**
- **Gain suppression mechanism in Low Gain Avalanche Detectors**
- **Setup extension to thin devices**
- **SEE studies in a RD53B chip**

Setup

M. Wiehe et al.:
Development of a Tabletop Setup for the Transient Current Technique
Using Two-Photon Absorption in Silicon Particle Detectors

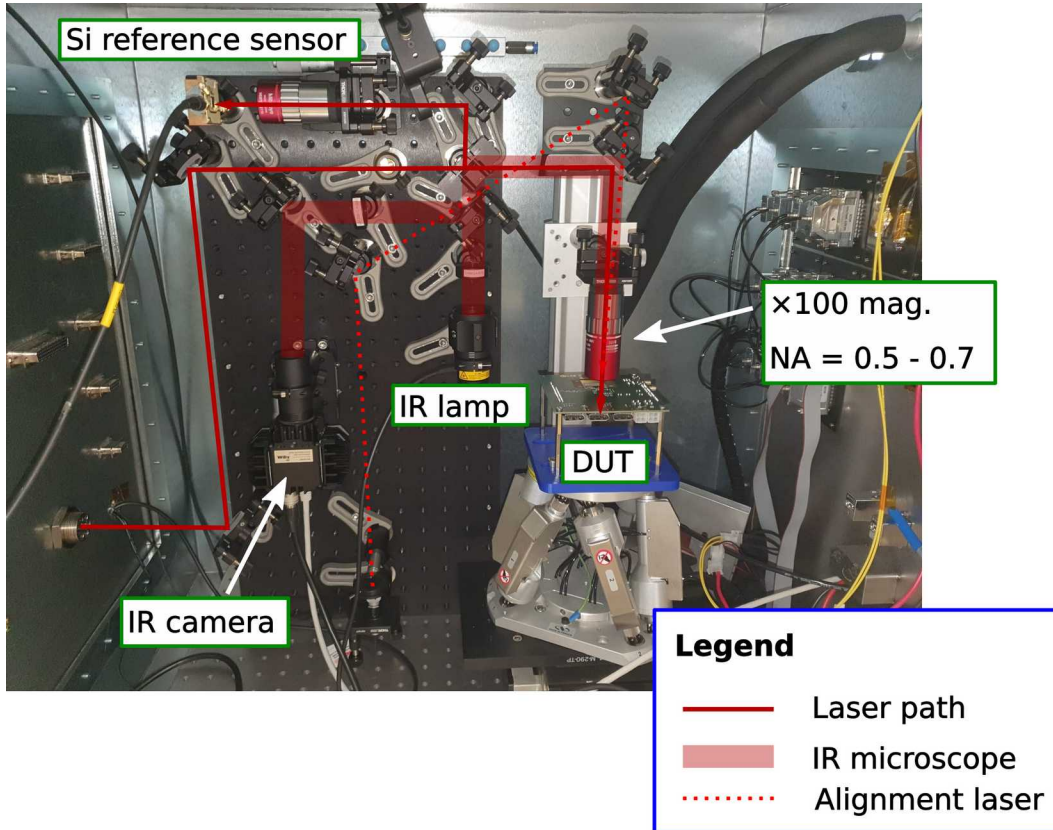


Laser output pulse properties:

- approx. 430 fs width
- pulse frequency 8 MHz to single pulse
- pulse energy up to 10 nJ
- central wavelength 1.55 μm

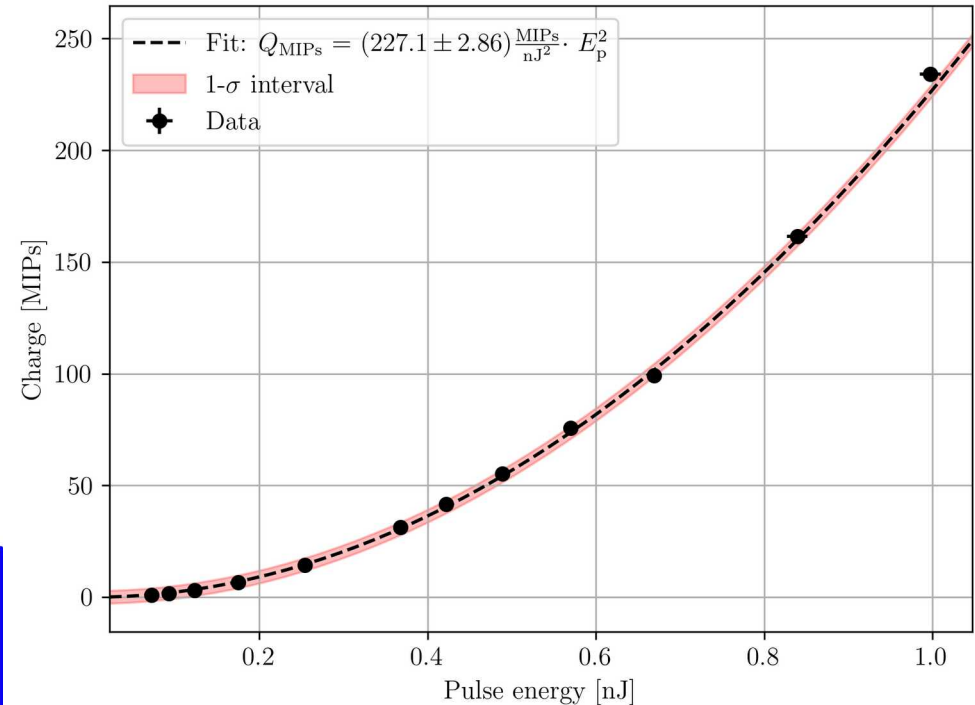
Setup

Inside of the Faraday cage:



Calibration:

Pulse energy vs generated charge (in a 300 μ m PIN with NA = 0.5 at 20 $^{\circ}$ C and 0% humidity):



Gain suppression mechanism

Gain suppression in gain devices

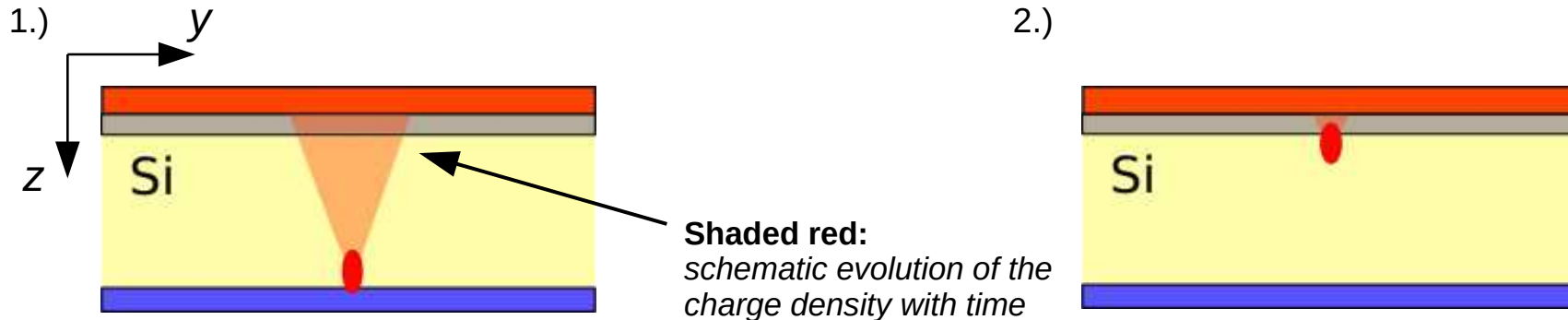
Comparison of β -source and TCT measurements of LGADs at CERN-SSD have shown that their gain depends on the charge density in the gain layer. This had not been realized until now.

- 1.) Low charge density in the GL will lead to a higher gain: there will be a negligible gain suppression.
- 2.) High charge density in the GL will lead to a reduction in the gain: drop in the GL E-field (less amplification).

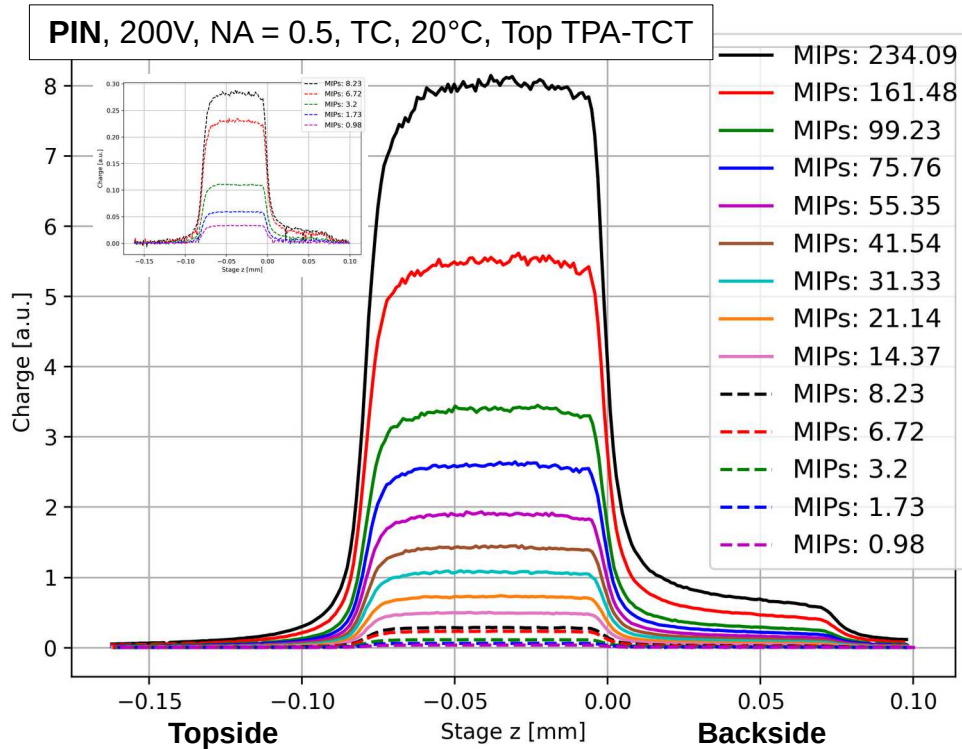
E. Currás - 38th RD50 Workshop

E. Currás, M. Fernández and M. Moll:
Gain suppression mechanism observed in Low Gain Avalanche Detectors (2021)

Idea behind gain suppression in TPA-TCT:



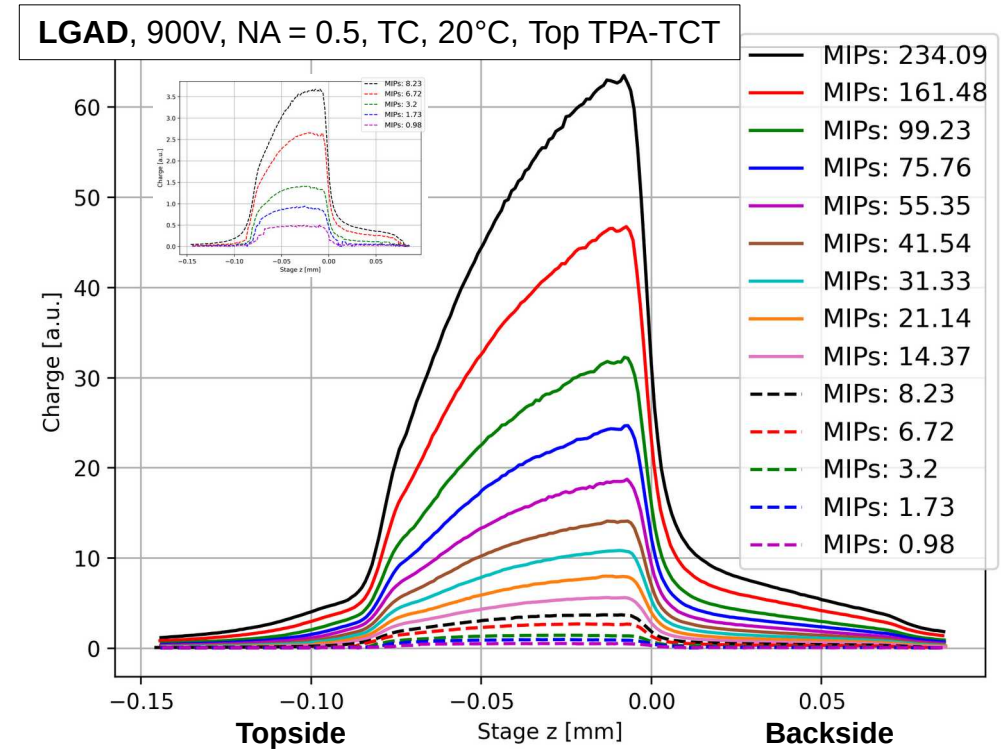
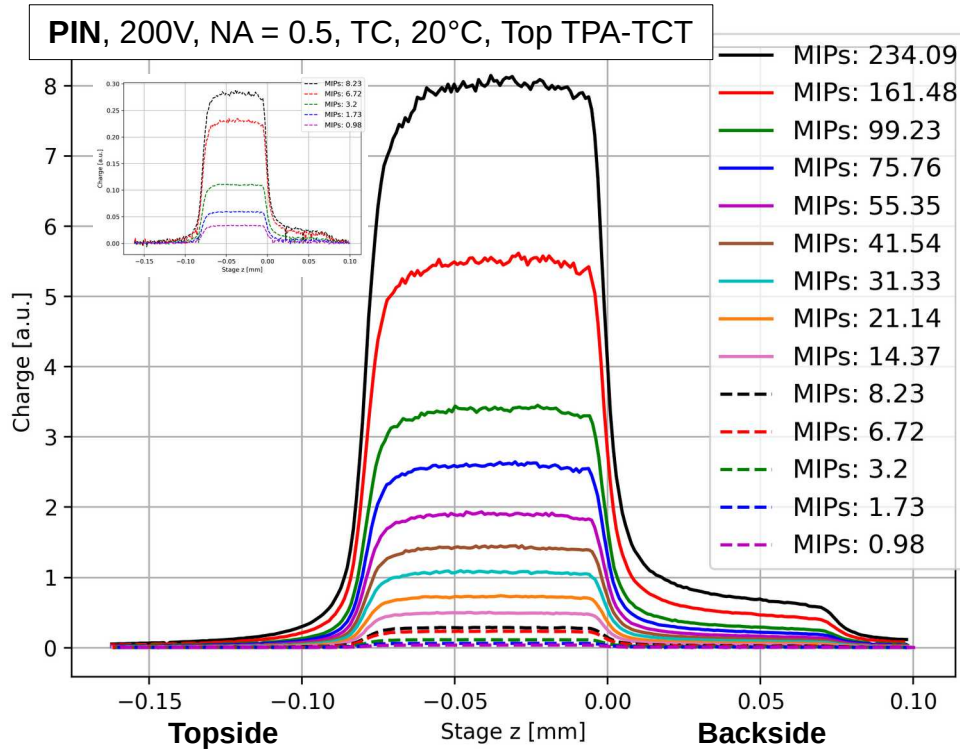
Charge collection: 280 μ m CNM PIN



Charge collection measurement in a PIN:

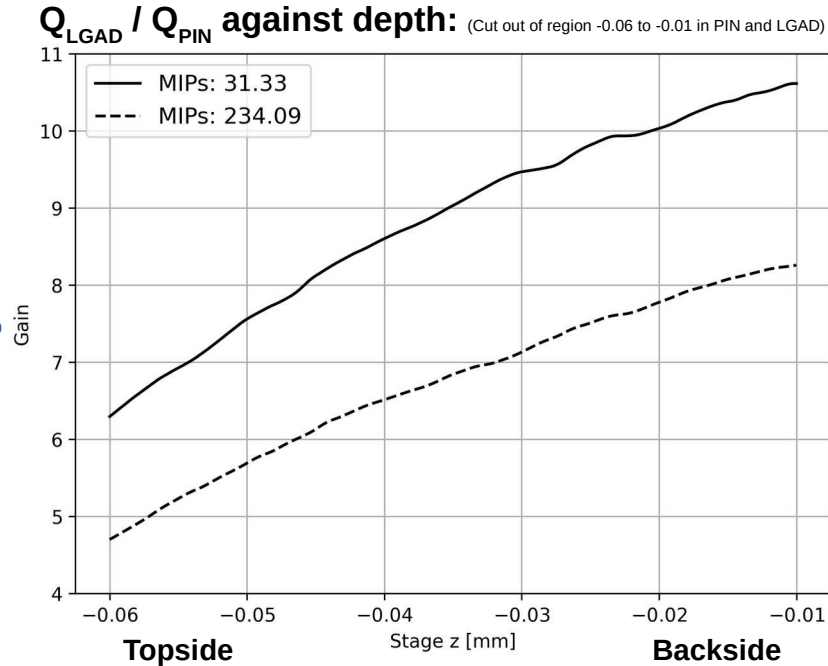
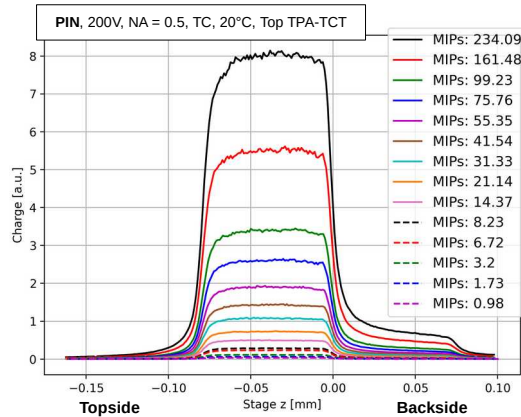
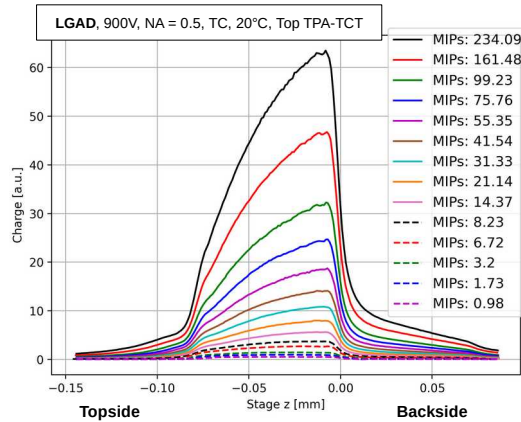
- behaves as expected
- Charge collection profile shape does not depend on the laser intensity / charge density.

Charge collection: 280 μm CNM PIN & LGAD



- Charge collection in a LGAD depends on laser intensity / charge density
- Gain suppression mechanism

Gain suppression: 280 μ m CNM LGAD



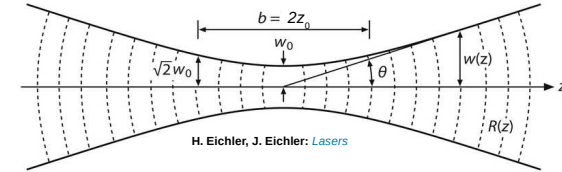
- Gain suppression increases with the charge carrier density
- lower in the backside because charge density decreases due to diffusion

Setup extension to thin devices

Highly focusing optics

It is found that for **thin devices** (50 - 70 μm) a higher focusing objective (NA = 0.7) improves the resolution, due to a smaller volume of charge generation. However, for thick devices a objective with NA = 0.5 is preferably used.

Beam parameter:

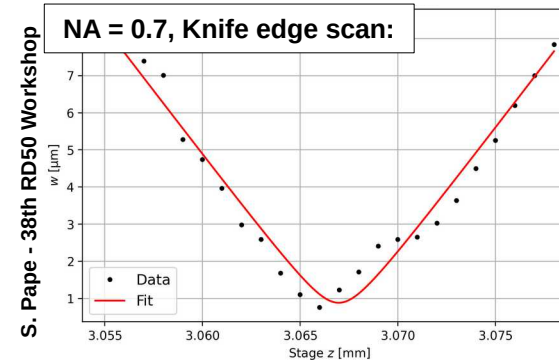
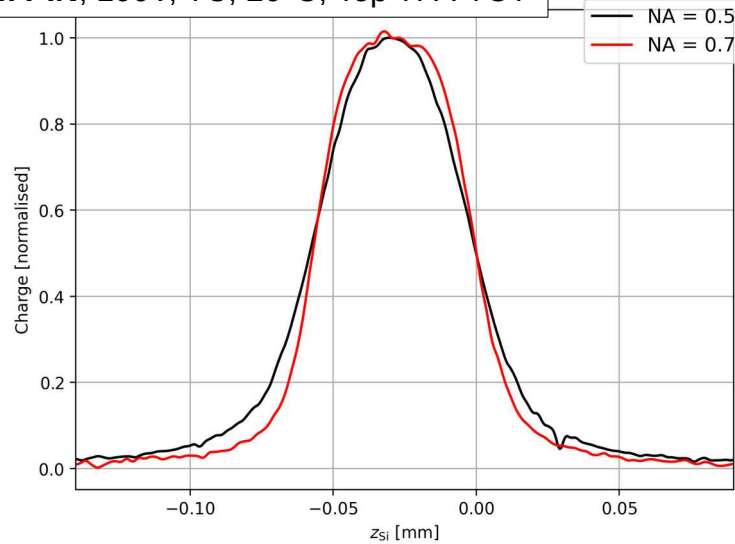


NA = 0.5: $w_0 = 1.3 \mu\text{m}$, $z_{0,\text{Si}} \approx 12 \mu\text{m}$

NA = 0.7: $w_0 = 0.9 \mu\text{m}$, $z_{0,\text{Si}} \approx 6 \mu\text{m}$

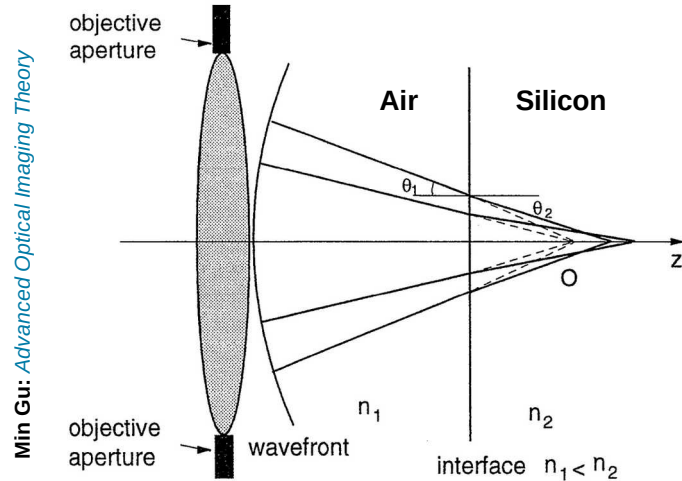
Charge collection in a 50 μm PIN measured with different NA:

~50 μm PIN, 100V, TC, 20 $^\circ\text{C}$, Top TPA-TCT



Rayleigh length for NA = 0.7 is approx. two times smaller
 → Volume of charge generation along the beam axis by a factor of two smaller

Aberration due to refractive index mismatch



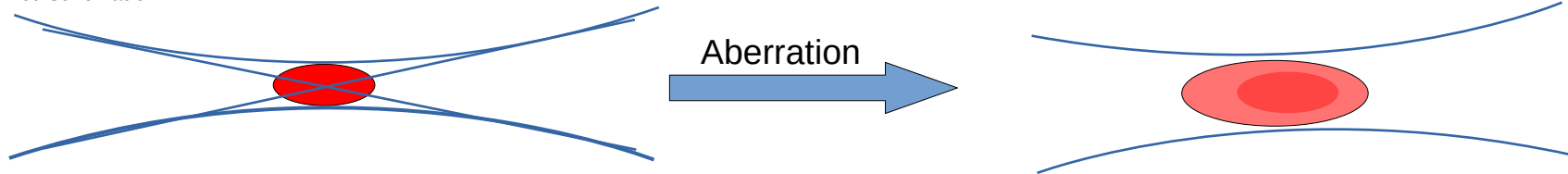
Aberration: light rays of different incident angles are focused at different positions on the axis

→ **The effect is linear with depth**

Mismatch of refractive indices at the top air-silicon interface ($n_1 = 1$, $n_2 = 3.4757$)

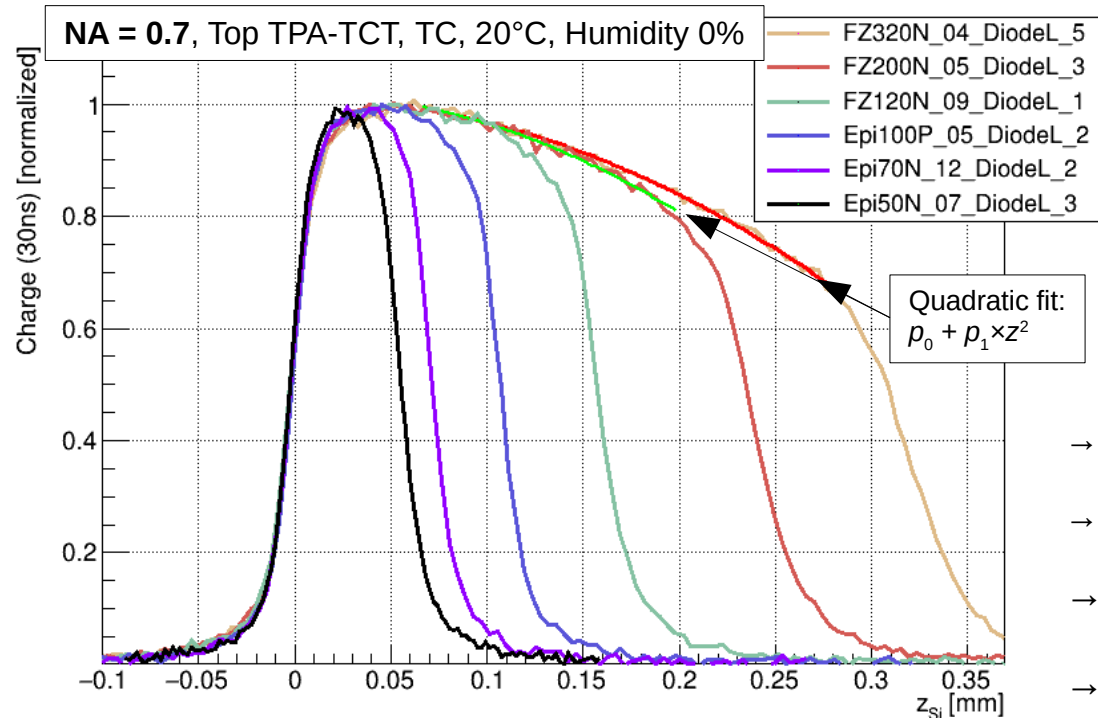
Aberration → defocused focal spot → lower intensity → less charge generation → linear effect → quadratic decrease in collected charge

Simplified schematic:



Charge Collection: numerical aperture 0.7

Measurements performed with an objective with a **numerical aperture** of **0.7** (not observed with NA = 0.5).
 Charge collection in PINs (HPK devices) with difference thicknesses:



- Orange: 320µm
- Red: 200µm
- Green: 120µm
- Blue: 100µm
- Purple: 70µm
- Black: 50µm

- Spherical aberration occurs with NA = 0.7 and leads to a distortion of the focal spot in depth
- Distortion visible for devices thicker than 70µm
- **Highly focusing objective (NA = 0.7) especially useful for thin devices**
- **Enables a more precise study of thin (segmented) silicon devices**

NA=0.7 → scaling factor 4.12

SEEs in the RD53B chip

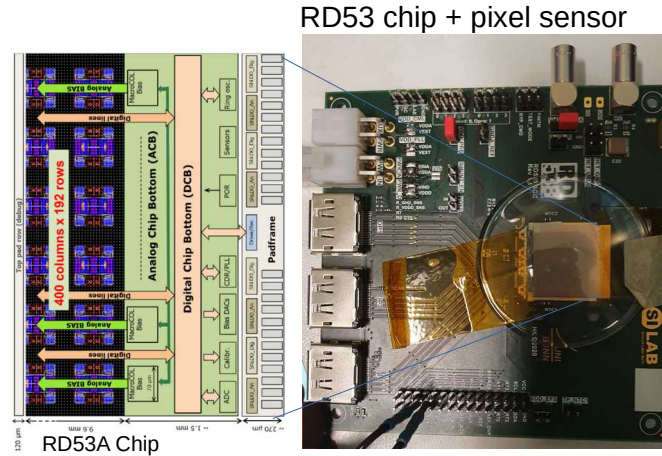
SEEs in RD53B Chip

Investigate SEEs in the RD53B chip in cooperation with CERN EP-ESE

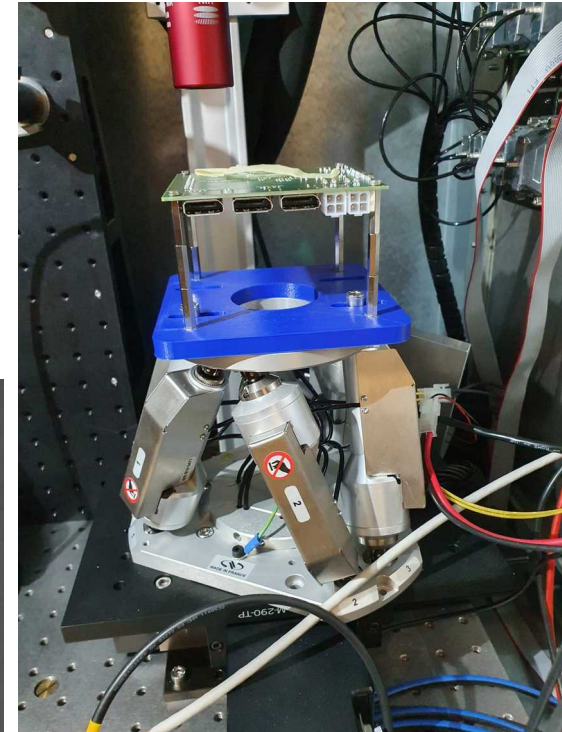
Measurements were before performed with a commercial TPA tool for SEE studies (Pulse Scan setup at Leuven).

Test CERN SSD TPA-TCT setup in comparison to the commercial SEE setup

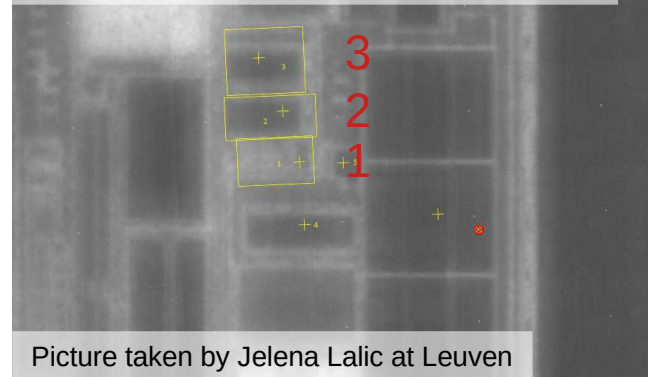
Simulations of the core bandgap region found SET → verified experimentally



RD53B chip mounted in the CERN SSD setup with a custom made holder:

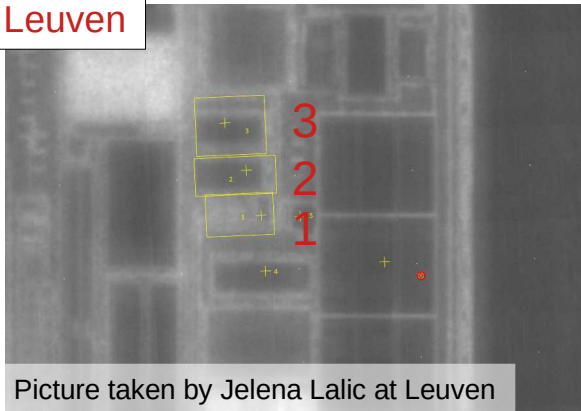


Transistors of the core bandgap (for Bias DAC) in the digital chip bottom:



SEEs in RD53B Chip: **Leuven** & **CERN SSD**

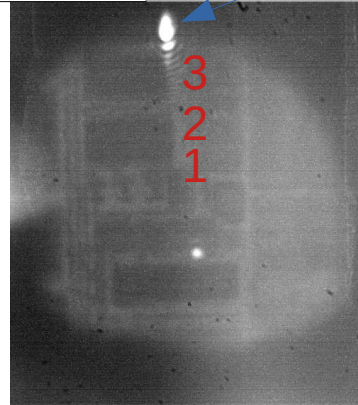
Leuven



Picture taken by Jelena Lalic at Leuven

CERN SSD

Laser beam spot



Charge injection in the transistor leads to SET event down the chain

CERN SSD setup reproduced first studies performed at **Leuven**.

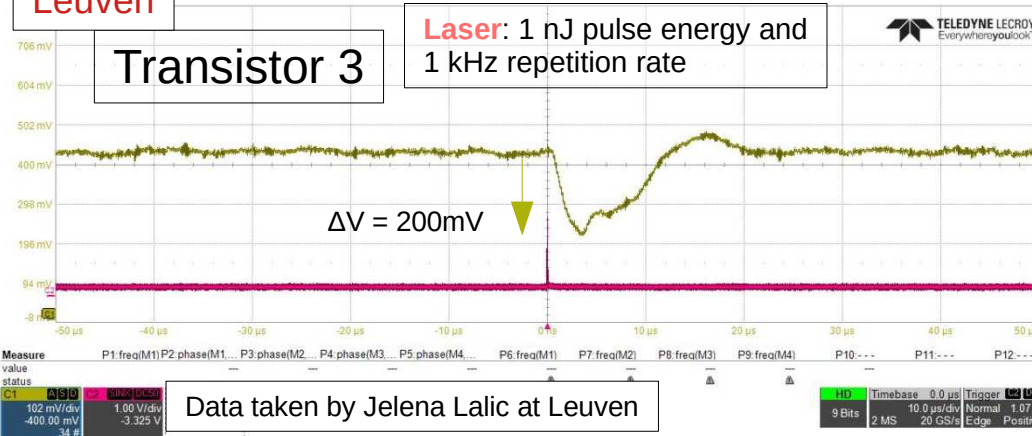
Not even full intensity used!
→ factor two in additional pulse energy possible

Leuven

Transistor 3

Laser: 1 nJ pulse energy and 1 kHz repetition rate

$\Delta V = 200\text{mV}$



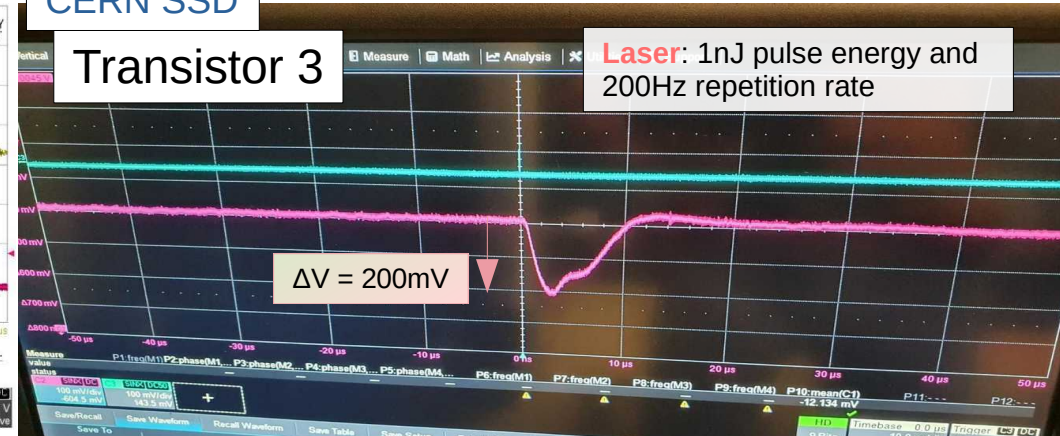
Data taken by Jelena Lalic at Leuven

CERN SSD

Transistor 3

Laser: 1nJ pulse energy and 200Hz repetition rate

$\Delta V = 200\text{mV}$



Summary

- Gain suppression mechanism was again verified using the TPA-TCT method
 - In depth study was performed → further analysis ongoing
- Highly focusing objectives ($NA = 0.7$) enable a more precise study of thin devices
 - $NA = 0.7$ limits the use to thin devices (approx. $\leq 70\mu\text{m}$), due to spherical aberration
 - spherical aberration **not observed with $NA = 0.5$**
- CERN SSD TPA-TCT setup suitable to perform SEE studies
 - Measurements performed in cooperation with CERN EP-ESE
 - First measurements at CERN SSD reproduced results from RD53



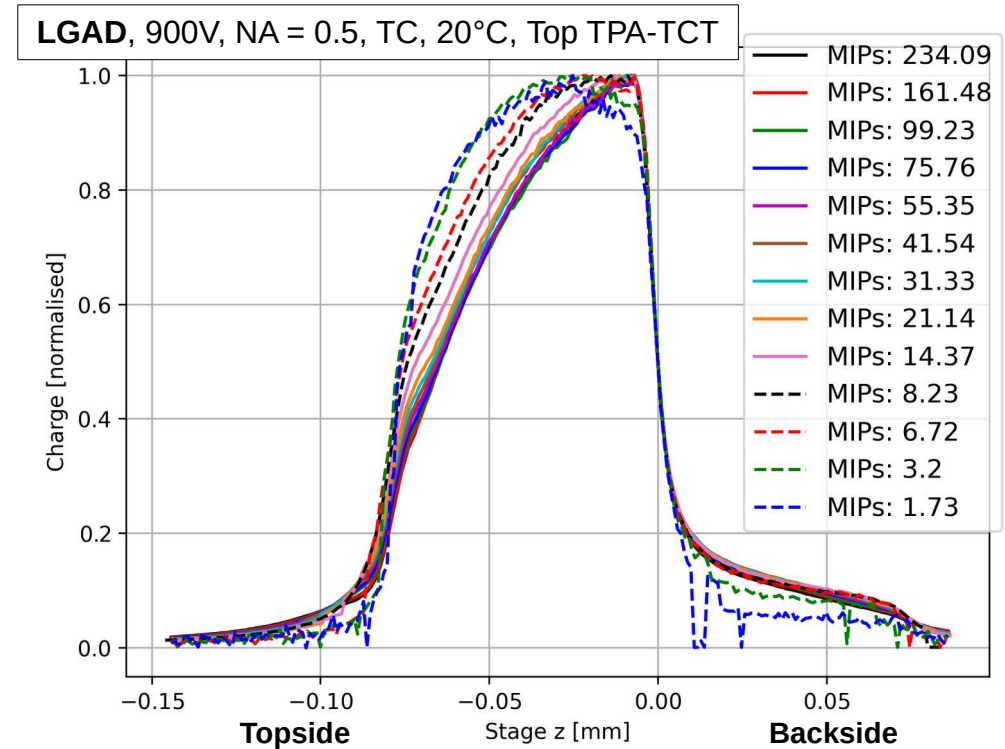
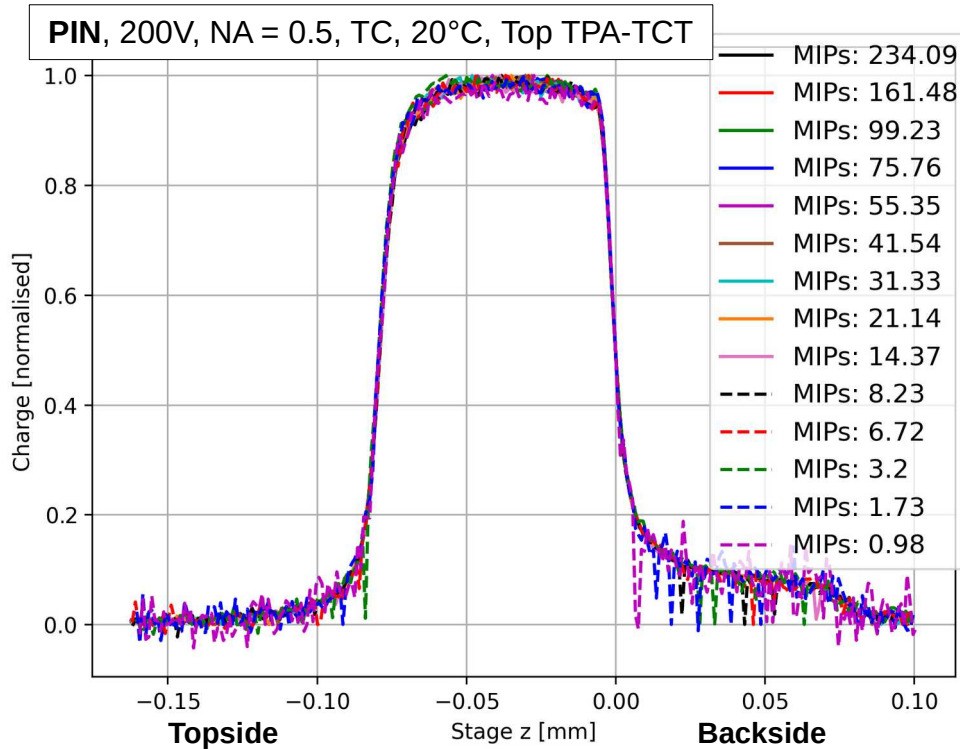
Thank you for your attention!



Federal Ministry
of Education
and Research

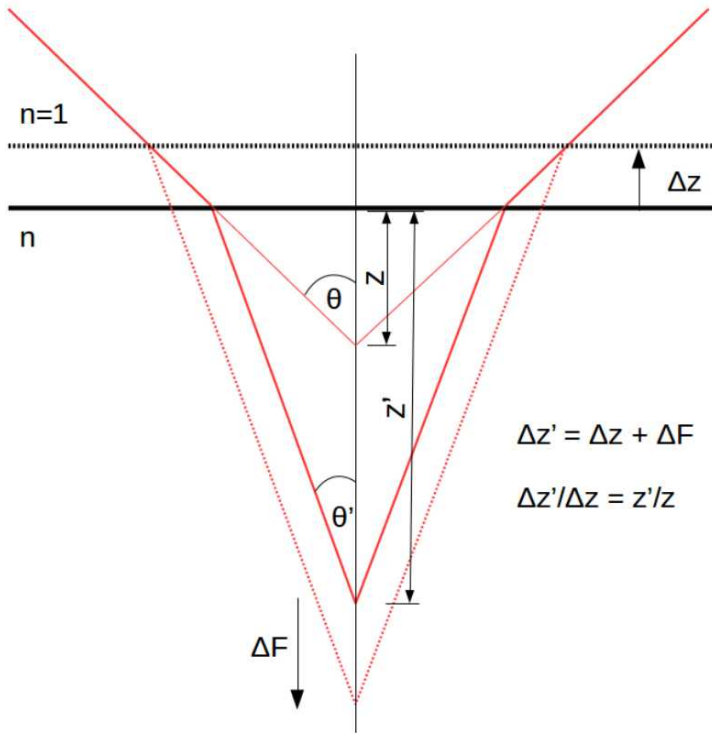
Backup

Charge collection: 280 μm CNM PIN & LGAD



- Charge collection in a LGAD depends on laser intensity / charge density
- Gain suppression mechanism

Refraction in silicon



M. Wiehe et al.: Development of a Tabletop Setup for the Transient Current Technique Using Two-Photon Absorption in Silicon Particle Detectors

Beam moves different in silicon than in air, due to refraction!

$$n_{\text{Si}} = 3.4757$$

Conversion of movement in air to movement in silicon depends on the focusing:

$$z' = z \sqrt{\frac{n^2 - NA^2}{1 - NA^2}}$$

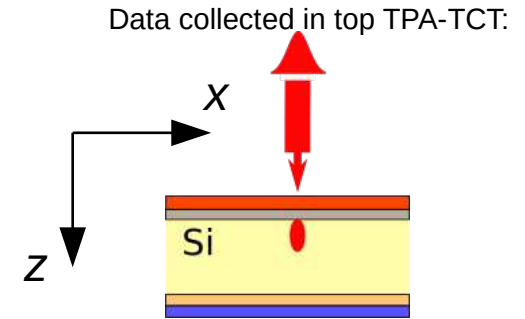
$$z' = z \sqrt{\frac{z_0 \pi n^3}{z_0 \pi n - \lambda n^2 + \lambda}}$$

Measured: $NA = 0.5 \rightarrow z'/z = 3.754$
 $NA = 0.7 \rightarrow z'/z = 4.12$

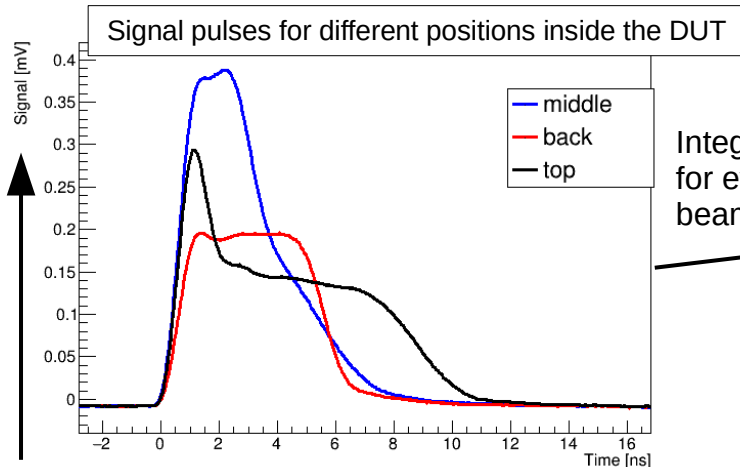
Prompt current method to extract the drift velocity

$$\sim v_{Drift}(z) = \mu(z) \approx -\mu I(\sim 0s)$$

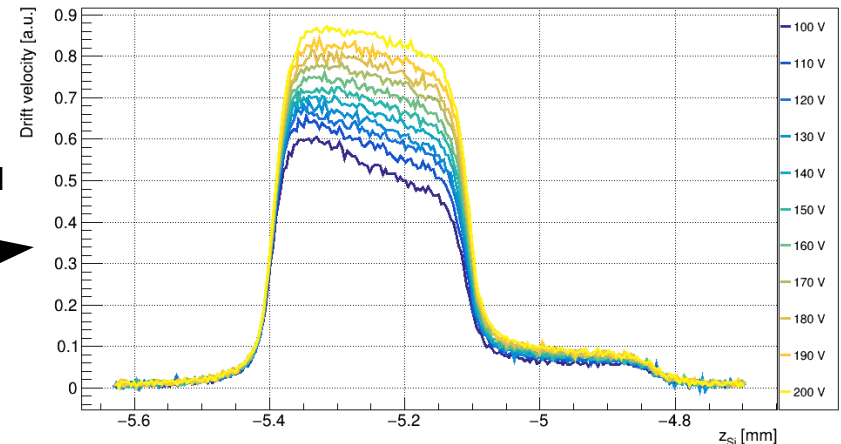
The drift velocity for a given z equals the charge carrier mobility (here holes) times the electric field at a given z value
 The electric field at a given z is correlated to the current signal at the time the laser generated the charge
 (Signal height and rise time contains information about electric field at the position where the charge is generated)



Integrate the first **600ps** of a signal pulse from a given z
 → estimator for the drift velocity $v_{Drift}(z)$, due to the above mentioned relation



Integrate the first 600ps signal for every z position of the beam's focal point

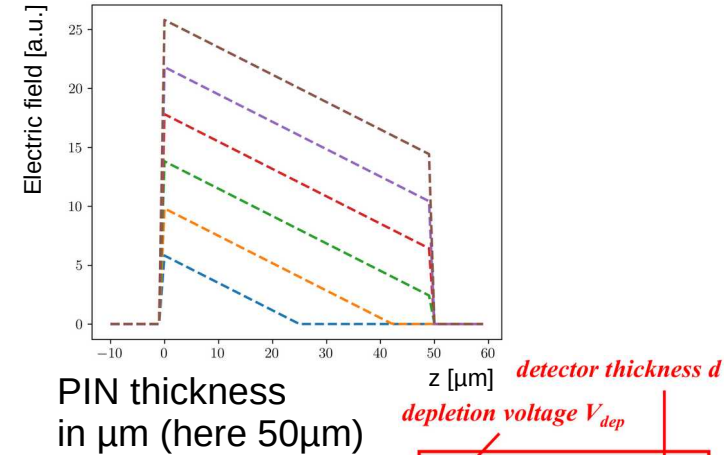


More details presented in: **G. Kramberger et al.:**
Investigation of Irradiated Silicon Detectors by Edge-TCT

Resolution: Charge profiles

$f(t)$ (PIN E-field):

Schematic depletion of a PIN:



$$V_{dep} = \frac{e}{2 \cdot \epsilon} \cdot |N_{eff}| \cdot d^2$$

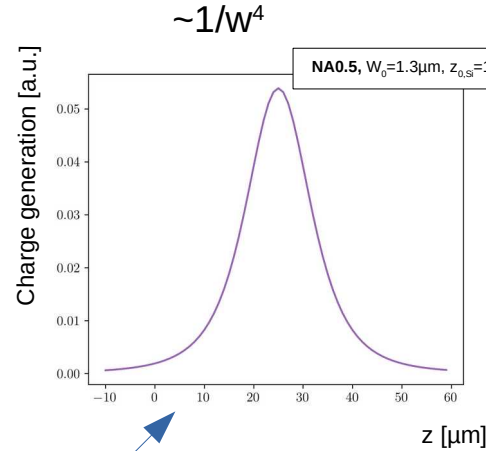
effective space charge density N_{eff}

M.Moll, SSD Meeting 01.03.2021

$$E(x) = \frac{1}{d} \cdot (V - V_{dep}) + \frac{2}{d} \cdot V_{dep} \cdot \left(1 - \frac{x}{d}\right)$$

$g(t)$ (Laser scanning function):

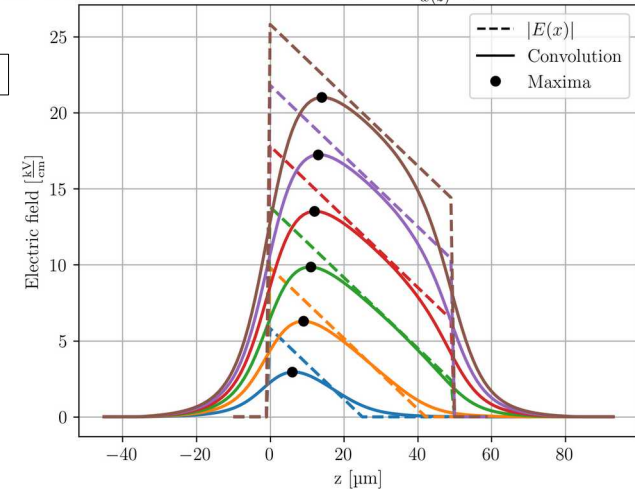
$$n_{tpa}(r, z) = \frac{E_p^2 \beta_2 4 \ln 2}{\tau \hbar \omega \pi^{\frac{5}{2}} w^4(z) \sqrt{\ln 4}} \exp\left[-\frac{4r^2}{w^2(z)}\right]$$



$1/w^4$ normalized by its integral

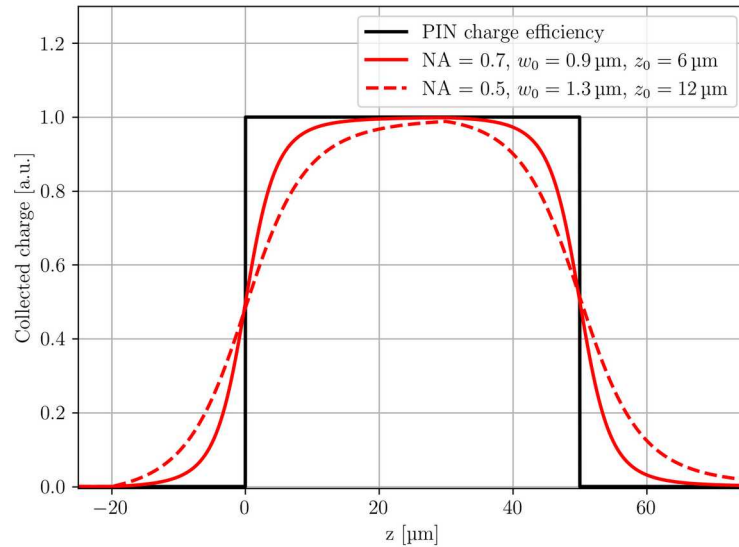
$$(f * g)(t) := \int_{-\infty}^{\infty} f(\tau)g(t - \tau) d\tau$$

Convolution of the electric field $|E(x)|$ with $\frac{1}{w(z)^2}$ ($w_0 = 1.3 \mu\text{m}$, $z_R = 12 \mu\text{m}$)

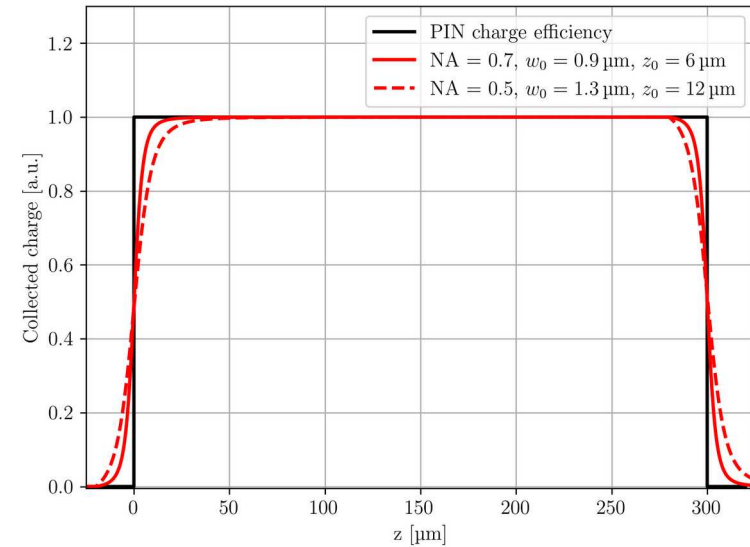


Theoretical comparison: NA 0.5 and NA 0.7

50 μm device



300 μm device



Spherical aberration not considered!